

## Nuclear equation of state and multi-messenger astronomy: Contribution of heavy-ion collisions

A. LE FÈVRE

*GSI Helmholtzzentrum für Schwerionenforschung GmbH - D-64291 Darmstadt, Germany*

received 26 November 2024

**Summary.** — In the past decade, new instruments in the field of multi-messenger astronomy like LIGO, VIRGO and NICER have provided great measurements. In the meanwhile, an increasing precision in the determination of the nuclear equation of state has been reached in the field of nuclear experiments. Altogether, they allowed breakthroughs in the knowledge of neutron star properties, and in bridging nuclear experimental constraints for symmetric matter and asymmetric nuclear matter to neutron stars. In particular, we demonstrate how constraints from heavy-ion collisions play a crucial role in neutron star studies. In the near future, improvements in transport models and nuclear theories, new accelerator facilities, new experiments, in conjunction with new neutron star measurements with enhanced precision should allow exploring the golden era of neutron star physics with heavy-ions collisions, by bridging further micro- and macroscopic collisions.

### 1. – Bridging micro- and macroscopic collisions

Due to their mass, neutron stars (NS) would undergo a gravitational collapse if they were not stabilised in a hydrostatic equilibrium by a repulsive pressure, made by the Fermi gas and strong interactions, that is described by the nuclear equation of state (EoS). Due to the density of neutron stars, of the order of magnitude of that of nuclei, the strong interaction plays a dominant role in their properties. Therefore, they are governed by the same strong interactions as in nuclei, whether it be in its crust —made of nuclei, electrons, clusters, superfluid neutrons—, or in its core —made of superfluid neutrons, superconducting protons, and eventually hyperons, deconfined quarks and color superconductor— [1], whose constituents and extreme conditions can be reproduced on Earth laboratory in heavy-ion collisions.

Sources to study the EoS of neutron stars are manifold. The microscopic composition (density dependence of the pressure and energy per nucleon, ...) in the interior of a neutron star determines its macroscopic properties (mass *vs.* radius) and vice versa, all linked to the EoS. On the microscopic level, the nuclear theory and heavy-ion collisions

help define what the EoS of a neutron star could be under various hypotheses (nucleonic, quark, hybrid or hyperon star), and therefore constrain macroscopic properties like its mass-radius and tidal polarisability. On the opposite side, on the macroscopic level, astrophysical events (gravitational waves, X-ray observations) allowing to determine the mass and radius of neutron stars permit to infer the density dependence of the pressure of those objects. This is done by calculating how much nuclear pressure is needed to counterbalance the gravitational pressure within general relativity for a given NS mass and radius, like defined, *e.g.*, by the Tolman-Oppenheimer-Volkoff (TOV) equation [2].

The main motivation of such trans-disciplinary approaches is to connect microscopic and macroscopic observations to extract the underlying EoS.

A pre-requisite for using heavy-ion collisions (HIC) to infer neutron star properties is that they are reproducing similar conditions of density and temperature as one finds in neutron stars, *i.e.*, rather dense (around 2–5 times saturation density  $\rho_0$ ), and rather cold. This implies HIC performed with rather large systems (in order to reach high densities) at intermediate incident energies ( $\approx 0.1$ – $10A$  GeV). At these energies, temperatures reached in the central fireball (participant region, of maximum compression and temperature) do not exceed those that are predicted in binary neutron star mergers [3].

Some analogies between nuclear (microscopic) and neutron star (macroscopic) properties are strongly related by the underlying EoS. For instance, the strength of the elliptic flow (squeeze-out) developed during HIC at intermediate energies, being correlated with the stiffness of the EoS translates into the tidal deformability in a neutron star. Moreover, the thickness of the neutron skin of neutron-rich nuclei is similarly correlated to the strength of the symmetry energy as the radius of a neutron star: a larger symmetry energy implies a thicker neutron skin for a given isotope, and a larger neutron star for a given mass.

## 2. – HIC achievements in constraining the nuclear EoS

The nuclear EoS is commonly expressed in terms of energy per nucleon as the sum of the symmetric nuclear matter ( $E_{SNM}$ ) component and the symmetry energy ( $E_{sym}$ ) in the following way:  $E(\rho, \delta) = E_{SNM}(\rho, \delta = 0) + \delta^2 E_{sym}(\rho) + O(\delta^4)$ , where  $\rho$  is the nucleonic density and  $\delta = \frac{\rho_n - \rho_p}{\rho_n + \rho_p}$  is the relative difference in density between neutrons and protons. In a neutron star  $\delta \approx 1$  because of the dominating neutron content. Therefore, to reconstruct its EoS, in addition to  $E_{SNM}$  one needs to determine  $E_{sym}$  whose contribution dominates the overall binding energy of a neutron star.

Historically, first determinations of the EoS from HIC experiments have concerned the density dependence of the SNM component, whose stiffness is commonly defined by the nuclear incompressibility modulus  $K_0 = 9\rho^2 \frac{\partial^2 E_{SNM}}{\partial^2 \rho} |_{\rho=\rho_0}$ . Various observables from HIC experiments have been used for constraining this parameter. In the pioneering experiment KaoS with the SIS synchrotron at GSI Darmstadt in the 1990s, kaon yields in central collisions have been used to conclude that the SNM EoS is rather soft, with  $K_0 \approx 200$  MeV [4]. Another powerful observable to constrain  $E_{SNM}$  is the flow of nucleons and clusters, that can be decomposed into a directed ( $v_1$ ) and an elliptic ( $v_2$ ) component. In the early ref. [5], the constraining power of  $v_1$  and  $v_2$  has been demonstrated at respectively high ( $> 2A$  GeV) and low ( $\lesssim 2A$  GeV) incident energies, from HIC experiments performed with the Bevalac accelerator at the Lawrence Berkeley National Laboratory and with the AGS synchrotron at the Brookhaven National Laboratory.

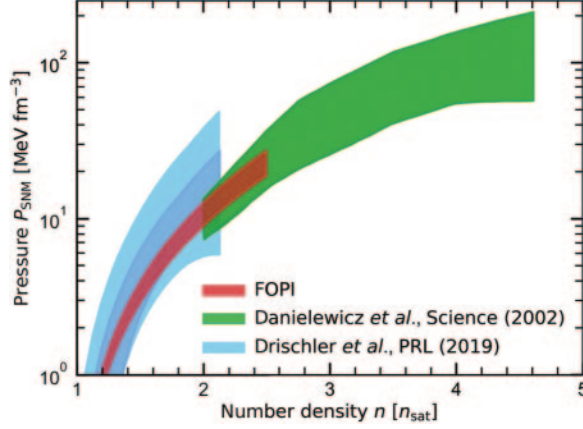


Fig. 1. – (Extracted from [6]). SNM EoS density dependence (in unit of saturation density) in terms of pressure, as constrained by various HIC experiments using flow observables: from refs. [5] (green) and [7] (red). The blue areas show  $\chi$ EFT nuclear theory predictions from refs. [8,9] at N2LO (light blue) and N3LO (dark blue).

This finding has been confirmed and precised by the FOPI Collaboration at GSI Darmstadt by studying the rapidity dependence of the elliptic flow of p, d, t,  $^3\text{He}$  in semi-central collisions of gold on gold, over a broad range of incident energies (0.1–1.5A GeV) [10]. Confronted to various transport model predictions, those data allowed to constrain the density dependence of  $E_{SNM}$  in the range  $0.7 < \rho/\rho_0 < 3$ , confirming its soft character with similar values of  $K_0$ :  $190 \pm 30$  MeV with IQMD [7],  $220 \pm 40$  MeV with UrQMD [11] and more recently  $230^{+9}_{-11}$  MeV with the dcQMD transport model [12]. Figure 1 shows the density dependence of the SNM EoS expressed in terms of pressure as resulting from analysis of refs. [5, 7], compared with nuclear theory expectations of the  $\chi$ EFT: they all show a fairly good agreement in their respective overlapping density ranges of validity.

Concerning the symmetry energy, HIC constraints came later. The first results concerned sub-saturation densities, from the analysis of isospin diffusion and isotope yields, confirming precise expectations from nuclear structure measurements (masses, isobaric analog states, neutron skin thicknesses, dipole polarisability) as shown in fig. 2(a) from the recent review of ref. [13].

Supra-saturation densities have been more recently constrained using again the elliptic flow observable, by comparing the flow of neutrons and light charged particles. This has been first achieved by the FOPI-LAND experiment [14] and improved afterwards by the ASY-EOS experiment [15] with gold on gold collisions at 400A MeV incident energy with the SIS accelerator at GSI Darmstadt. Densities probed in these experiments range between 0.7 and  $2\rho_0$ . These data favour a rather soft  $E_{sym}(\rho)$ , with a slope parameter  $L = 3\rho_0 \frac{\partial E_{sym}}{\partial \rho} |_{\rho=\rho_0}$  ranging between  $63 \pm 11$  and  $72 \pm 13$  with  $E_{sym}(\rho_0) = 31$  and 34 MeV, respectively, as hypothesis, according to the UrQMD transport model. Resulting constraints on the density dependence of  $E_{sym}$  are shown in fig. 2(b). As in panel (a), we note that the sub-saturation density extension of the ASY-EOS constraint is in agreement with previously mentioned nuclear experimental results. Further analyses of these data with other transport models have led to similar conclusions [13], in particular in a more

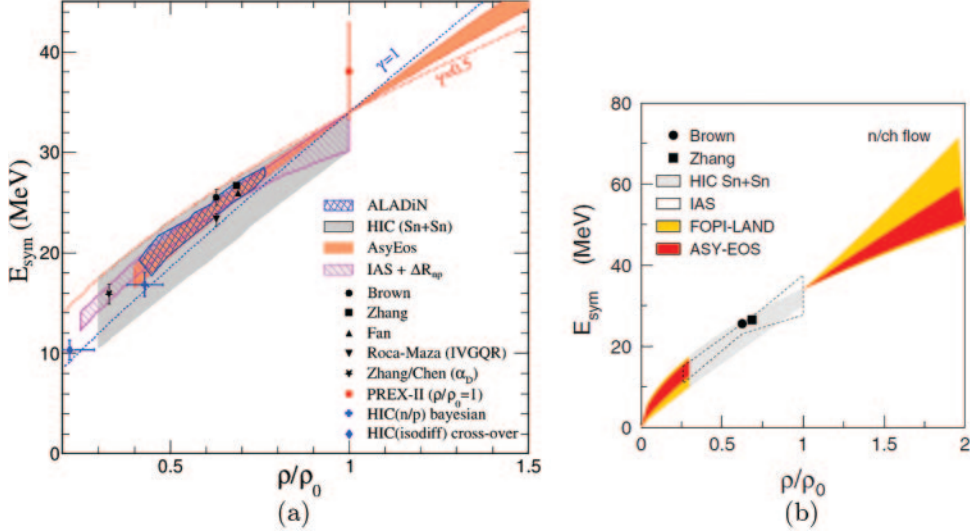


Fig. 2. – (Extracted from [13] —see this reference for details). (a) Symmetry energy dependence in sub-saturation densities as deduced from nuclear structure measurements (black and red markers) and HIC (shaded areas and blue markers). (b) Density dependence of the symmetry energy deduced from the elliptic flow ratio of neutrons and hydrogen isotopes in the ASY-EOS (orange band) and FOPI-LAND (yellow band) experiments, compared also to some low-density HIC and nuclear structure measurements displayed in panel (a).

recent and refined analysis with the dcQMD model [12], concluding with  $L = 63_{-13}^{+10}$  MeV and  $E_{sym}(\rho_0) = 35 \pm 1$  MeV.

Another way to probe the symmetry energy at high density with HIC is to measure the  $\pi^+$  over  $\pi^-$  yield ratio of pions emitted in central collisions at near sub-threshold incident energies. At these energies, densities probed by the observable are about  $1.5\rho_0$  [16]. This has been achieved by FOPI experiments more than a decade ago [17, 18], concluding that the density dependence of  $E_{sym}$  is soft or eventually super-soft. More recently, the S $\pi$ RIT experiment at RIKEN has confirmed these findings, with  $42 < L < 117$  MeV [19]. However, the constraining power of the pion observable is remaining smaller than that of the elliptic flow, and particularly model dependent.

### 3. – Why HIC are needed for neutron star studies

As we will see later, HIC have the capability to inform the EoS of a neutron star in density regions where present multi-messenger astronomy (gravitational waves, X-ray observations, ...) is weakly constraining, whether it be for modelling the crust, or for getting a precise mass-radius relation for which low to intermediate densities ( $1 - 3\rho_0$ ) are crucial [20,21]. The same applies as well concerning the relation between the tidal deformability of a neutron star and its radius: without high density HIC constraints on the EoS, uncertainties are much larger [22]. Whereas the constraint on the maximum mass of neutron stars and radio pulsar observations influence the determination of the EoS only above  $4\rho_0$ , gravitational wave and X-ray timing measurements have little influence on the EoS below  $2\rho_0$  [23]. In addition, the most significant densities for constraining

neutron star radii are believed to be about  $1.5-2\rho_0$  and  $2-3\rho_0$  for respectively 1.4 and 2 solar mass ( $M_\odot$ ) neutron stars [23,24].

#### 4. – A new era of combining HIC to astronomical findings

Up to recent years, the only EoS inputs from nuclear physics that were used to constrain neutron star properties are the chiral effective field theory ( $\chi$ EFT) [8, 25], deductions from giant dipole resonance experiments and nuclear neutron skin measurements [26]. Unfortunately, these inputs are only valid near sub-saturation densities, whereas neutron star properties like their mass-radius relation and tidal deformability are mainly sensitive to larger densities ( $> 1.5\rho_0$ ). This implies extrapolations diminishing the accuracy of nuclear physics inputs.

A first attempt to use the EoS constraints from HIC (FOPI and ASY-EOS), covering larger densities, in conjunction with astronomical multi-messenger observations

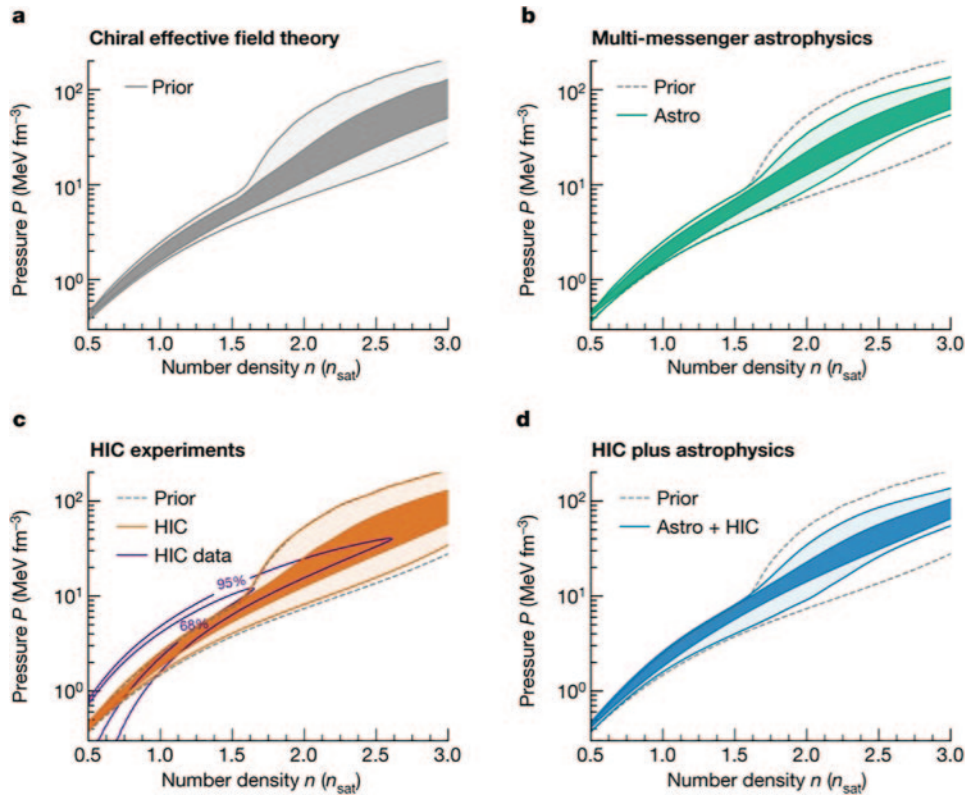


Fig. 3. – (Extracted from [6]). Constraints on the EoS of neutron star matter. (a)–(d): evolution of the pressure as a function of baryon number density for the EoS prior used for the Bayesian analysis ((a) grey), when including only data from multi-messenger neutron star observations ((b) green), when including only HIC data ((c) orange), and when combining both ((d) blue). The shading corresponds to the 95% and 68% credible intervals (lightest to darkest). The impact of the HIC experimental constraint (HIC data, purple lines at 95% and 68%) on the EoS is shown in (c). In (b)–(d), the 95% prior bound is shown for comparison (grey dashed lines).

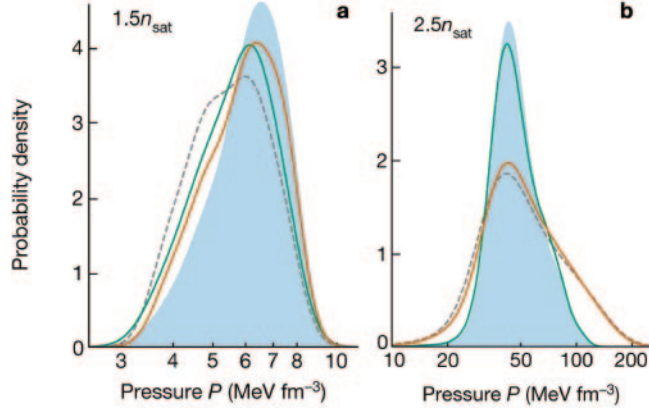


Fig. 4. – (Extracted from [6]). Posterior distributions for the pressure in neutron star matter at  $1.5\rho_0$  (a) and  $2.5\rho_0$  (b) with various inputs of the Bayesian analysis, with the result of combined Astro + HIC shaded in light blue; lines: see legend of fig. 3.

(kilonovas, X-ray and gravitational waves) has been successfully made by Huth, Pang *et al.* [6], within a Bayesian analysis framework. It has proven that HIC can be as accurate as astronomical measurements for constraining the EoS of neutron star matter. The other remarkable finding is that both agree in their common range of explored density. Figure 3 shows the EoS deduced in this work from various inputs. In particular, panel (d) represents the final EoS constraints obtained by combining both astrophysical multi-messenger observations and HIC information. We see that whereas astrophysical data rule out the most extreme EoS’s, HIC inputs indicate larger pressures around  $1\text{--}1.5\rho_0$ , the density range where the HIC (ASY-EOS) experimental sensitivity is the highest. This supports recent NICER observations on the EoS [27, 28]. As illustrated by fig. 4 (panel (a)), HIC experiments and astronomical observations (“Astro”) show an almost perfect agreement. At low densities (panel (a)), HIC exhibit a clear impact on the posterior (Astro+HIC combined) EoS distribution, having an accuracy comparable to that of astronomical inputs. At higher density ( $\geq 2\rho_0$ ), where  $E_{sym}$  determined from HIC is less accurate, the EoS combination is mostly determined by astronomical observations (panel (b)). As astronomical observations mainly probe neutron stars with  $M \geq 1.4M_\odot$ , for which the relevant densities are higher than those probed by ASY-EOS, HIC inputs used in this study influence the radii of these neutron stars to a smaller degree, improving slightly their accuracy. Present HIC data start to have some influence on radii of low-mass stars with  $M \approx 1.0 M_\odot$ .

Similar findings have been later confirmed by Tsang *et al.* [29], using non-parametric equations of state as priors instead of  $\chi$ EFT. One of their conclusions is that when using a Bayesian method, the choice of the prior plays a strong role in density regions where its variation range is narrow, which may represent a bias when uncertainties of this prior are underestimated. In comparison to their more liberal prior, the  $\chi$ EFT used in [6] forces the posterior EoS to be softer in the  $1\text{--}1.5\rho_0$  density range.

In a similar Bayesian approach, Koehn *et al.* [30] have recently confirmed the radius of  $1.4M_\odot$  neutron stars found in Huth *et al.* [6] ( $12.01 \pm 0.78$  km) with  $12.20 \pm 0.53$  km, using 100000 EoS’s from metamodeling and a speed of sound extension up to  $25\rho_0$ .

## 5. – Perspectives: towards higher densities and precision

As seen previously, whereas the highest densities probed by HIC for the SNM EoS are about  $3\text{--}4\rho_0$ , the validity of the symmetry energy constrained by HIC does not go beyond  $1.5\rho_0$ , which represents the limiting frontier of HIC for predicting the EoS of neutron star matter. In order to extend this frontier up to about  $2.5\rho_0$ , a new experimental campaign, ASY-EOS II, is planned at GSI Darmstadt in Spring 2025, still with Au + Au collisions, within the R3B Collaboration [13,31]. Like for the first campaign (cf. sect. 2), the flow ratio method will be employed. Here, thanks to the New Large-Area Neutron Detector (NeuLAND), unlike during the first experiment, protons will be discriminated from other light charged isotopes, allowing to measure the elliptic flow ratio of neutrons and protons, which is predicted to probe higher densities than with mixing all hydrogen isotopes, as illustrated by fig. 5 (left panel). In addition, in this new experiment, a large set of bombarding energies will be used (250, 400, 800A MeV). Whereas the lowest energy (250A MeV) is supposed to best constrain the curvature ( $K_{sym} = 9\rho_0^2 \frac{\partial^2 E_{sym}}{\partial^2 \rho} |_{\rho=\rho_0}$ ) of the symmetry energy [32], the highest one (800A MeV), twice as large as in the previous experiment (400A MeV) is expected to probe larger densities as illustrated by fig. 5 (right panel). Finally, a better accuracy of the determination of the reaction plane is expected, which should reduce uncertainties of the extracted symmetry energy.

In a more distant future, other experimental programs using HIC aim at constraining further  $E_{sym}$  at high densities, above  $3\rho_0$ , like CBM and HADES at FAIR (Darmstadt) with the future SIS100 accelerator, with higher bombarding energies (up to  $\approx 10A$  GeV).

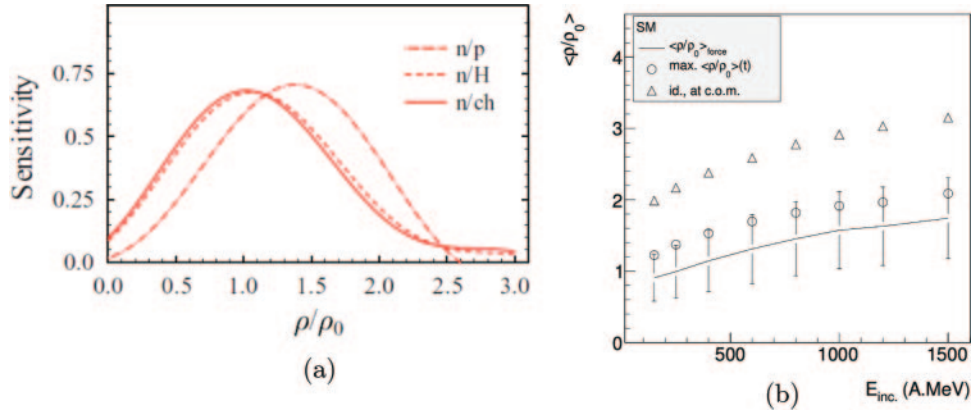


Fig. 5. – (Extracted from [13] –see this reference for details). (a) TüQMD transport model predictions for the ratio of elliptic flows of neutrons and charged particles for the Au+Au system at 400A MeV: sensitivity density (solid line) together with the ones obtained from elliptic-flow ratios of neutrons over all hydrogen isotopes (dashed line) and neutrons over protons (dash-dotted line) [15]. (b) IQMD transport model predictions of the incident energy dependence of the average reduced density  $\langle \rho/\rho_0 \rangle$  of protons in semi-central collisions of Au + Au, for various space-time selections: (triangles) maximum value reached in the central volume of the collision, (circles) maximum value for protons ending-up at mid-rapidity and large transverse momentum, similarly to the ASY-EOS acceptance (reduced transverse velocity  $ut_0 > 0.4$  and reduced rapidity  $|y_0| < 0.8$ ), (error bars) spread distribution (one sigma) of the time averaged value weighted by the force of the mean field felt by protons falling in the same phase space selection [7, 33].

Both detectors have the capability to measure with an unprecedented precision meaningful observables for the determination of the nuclear EoS, like flows, sub-threshold particle yields, and di-leptons. Di-leptons inform on temperatures reached at the maximum compression phase of the colliding system. Flows can be informative on the compressibility of the system up to highest SIS100 beam energies, probing densities up to  $\approx 7\rho_0$ , as shown by Danielewicz *et al.* [5]. With SIS100 higher beam energies, similarly to sub-threshold pions measured at lower bombarding energy (see sect. 2), new pairs of isospin conjugate particles emitted at sub-threshold energy are promising good candidates for constraining  $E_{sym}$ . For instance with  $K^+ / K_0$  [34] and  $\Sigma^- / \Sigma^+$  [35] yield ratios. Both sigma and kaon mesons are expected to carry the  $E_{sym}$  density dependence since their production is dominated by primordial pions. Similarly, the doubly strange baryon ratio  $\Xi^- / \Xi^0$  is expected by Yong *et al.* [35] to have the strongest sensitivity to the variation of  $E_{sym}$  at high density, for  $\sqrt{s_{NN}} \approx 3$  GeV incident energies. However, in order to make these observables conclusive, high counting rates and small transport model uncertainties are crucial as shown by Lopez *et al.* [34] from a pioneering FOPI experiment at GSI where both the statistics and model uncertainties did not allow to draw conclusions on the stiffness of the asymmetry potential density dependence.

The existence of a quark-gluon plasma (QGP) phase transition and the density dependence of the hyperon-nucleon potential are two other meaningful pieces of information that HIC experiments have the potential to provide, which are fundamental for the determination of neutron star EoS at very large densities ( $\gg 4\rho_0$ ), up to the perturbative QCD limit.

The constraining power of the afore-mentioned observables is depending on the first order of the accuracy of transport models that are used to simulate collisions. Therefore, much effort must be invested on transport modelling improvements and bench-marking, as pursued by the Transport Model Evaluation Project [36], and in the comprehensive review publication of Sorensen *et al.* [37]. Furthermore, as needed by external scientific communities and scholar textbooks, one could expect from such collaborative works a world consensus delivering a common HIC EoS, with well-defined errors, consistent with all transport codes.

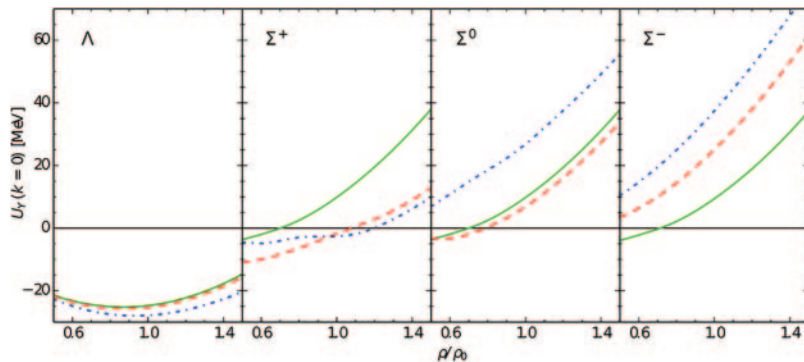


Fig. 6. – (Extracted from [41]). Predictions from  $\chi$ EFT at NLO (next leading order) with a cutoff  $\Lambda = 600$  MeV for the density dependence of the hyperon (at rest) single-particle potentials with different compositions of the nuclear matter. The green solid, red dashed and blue dash-dotted curves are respectively for isospin-symmetric nuclear matter, asymmetric nuclear matter with  $\rho_{protons} = 0.25\rho$  and pure neutron matter.

On the front of nuclear theory, like  $\chi$ EFT, parallel efforts are foreseen to improve the accuracy of the description of the nuclear EoS, and in particular of pure-neutron matter, at supra-saturation densities. As suggested by Tsang *et al.* [29],  $\chi$ EFT errors are probably still too optimistic at supra-saturation densities in comparison with the neutron star matter EoS expectations coming from both astronomical multi-messenger observations and HIC experiments. In order to be able to treat consistently larger densities,  $\chi$ EFT must deal with various degrees of freedom (N, $\pi$ , $\Delta$ ,Y, ...), and must offer controlled uncertainty estimates. Several recent promising works are trying to see how high in density can one push the  $\chi$ EFT, by involving the role of Delta resonances and hyperons [38-41]. In particular, they offer predictions of the hyperon in-medium potential density dependence, shown in fig. 6 by Petschauer *et al.* [41], that could be benchmarked by future HIC experiments at FAIR and NICA aiming at probing the hyperonic in-medium properties.

## 6. – Conclusion

In the past decade great new astronomical instruments like LIGO/VIRGO and NICER have provided great measurements, and major improvements in the understanding of neutron star properties. In parallel, on the HIC side, breakthroughs which connect experimental constraints for symmetric matter and asymmetric matter to neutron stars have been achieved.

In the near future, further improvements and breakthroughs in transport model simulations and nuclear theory are expected. In the coming decade, a new generation of gravitational wave detectors, about 10 times more sensitive, should allow probing the post-merger neutron-star physics [42], *i.e.*, larger densities where a possible QGP transition should be observed if ever existing. The reach of the Cosmic Explorer 40 km observatory for compact binary mergers is expected to probe much (further) older neutron-star mergers, thanks to an improved signal/noise ratio, increasing by far the event statistics, therefore the precision of the EoS and mass-radius constraint of neutron star matter.

Improvements of the symmetry energy constraints below  $3\rho_0$  are expected with the second ASY-EOS experiment at GSI in 2025, and other new HIC experiments planned for the coming decade (CBM/HADES/R3B@FAIR, BM@N, FRIB, RIKEN, ...) at new accelerator facilities (FRIB400, FAIR, NICA) should allow improving the EoS accuracy and pushing its knowledge above  $3\rho_0$ , with the help of improved transport models and nuclear theories.

This opens the perspective of exploring the golden era of neutron star physics with HIC.

## REFERENCES

- [1] WATTS A. L. *et al.*, *Rev. Mod. Phys.*, **88** (2016) 021001.
- [2] OPPENHEIMER J. R. and VOLKOFF G. M., *Phys. Rev.*, **55** (1939) 374.
- [3] HANAUSKE M. *et al.*, *J. Phys.: Conf. Ser.*, **878** (2017) 012031.
- [4] STURM C. *et al.*, *Phys. Rev. Lett.*, **86** (2001) 39.
- [5] DANIELEWICZ P. *et al.*, *Science*, **298** (2002) 1592.
- [6] HUTH S. *et al.*, *Nature*, **606** (2022) 276.
- [7] LE FÈVRE A. *et al.*, *Nucl. Phys. A*, **945** (2016) 112.
- [8] DRISCHLER C. *et al.*, *Phys. Rev. Lett.*, **122** (2019) 042501.
- [9] LEONHARDT M. *et al.*, *Phys. Rev. Lett.*, **125** (2020) 142502.

- [10] REISDORF W. *et al.*, *Nucl. Phys. A*, **876** (2012) 1.
- [11] WANG Y. *et al.*, *Phys. Lett. B*, **778** (2018) 207.
- [12] COZMA D., *Equation of state of nuclear matter from collective flows and stopping in intermediate energy heavy-ion collisions*, to be published in *Phys. Rev. C* (2024) arXiv:2407.16411 [nucl-th].
- [13] RUSSOTTO P. *et al.*, *Riv. Nuovo Cimento*, **46** (2023) 1.
- [14] RUSSOTTO P. *et al.*, *Phys. Lett. B*, **697** (2011) 471.
- [15] RUSSOTTO P. *et al.*, *Phys. Rev. C*, **94** (2016) 034608.
- [16] LYNCH W. and TSANG M., *Phys. Lett. B*, **830** (2022) 137098.
- [17] REISDORF W. *et al.*, *Nucl. Phys. A*, **781** (2007) 459.
- [18] XIAO Z. *et al.*, *Phys. Rev. Lett.*, **102** (2009) 062502.
- [19] ESTEE J. *et al.*, *Phys. Rev. Lett.*, **126** (2021) 162701.
- [20] RAITHEL C. A. and MOST E. R., *Phys. Rev. Lett.*, **130** (2023) 201403.
- [21] RAITHEL C. A. and MOST E. R., *Phys. Rev. D*, **108** (2023) 023010.
- [22] KUMAR ROHIT, private communication, work in progress.
- [23] LEGRED I. *et al.*, *Phys. Rev. D*, **104** (2021) 063003.
- [24] ANNALA E. *et al.*, *Phys. Rev. Lett.*, **120** (2018) 172703.
- [25] HEBELER K. and SCHWENK A., *Eur. Phys. J. A*, **50** (2014) 11.
- [26] LATTIMER J. M., *J. Phys.: Conf. Ser.*, **2536** (2023) 012009.
- [27] MILLER M. C. *et al.*, *Astrophys. J. Lett.*, **918** (2021) L28.
- [28] RAAIJMAKERS G. *et al.*, *Astrophys. J. Lett.*, **918** (2021) L29.
- [29] TSANG C. Y. *et al.*, *Nat. Astron.*, **8** (2024) 328.
- [30] KOEHN H. *et al.*, *From existing and new nuclear and astrophysical constraints to stringent limits on the equation of state of neutron-rich dense matter*, arXiv:2402.04172 [astro-ph.HE] (2024).
- [31] RUSSOTTO P. *et al.*, *Symmetry energy at high densities from neutron/proton flow excitation functions*, arXiv:2105.09233 [nucl-ex] (2021).
- [32] COZMA M. D., *Eur. Phys. J. A*, **54** (2018) 40.
- [33] LE FÈVRE A. *et al.*, *Phys. Rev. C*, **98** (2018) 034901.
- [34] LOPEZ X. *et al.*, *Phys. Rev. C*, **75** (2007) 011901.
- [35] YONG G.-C. *et al.*, *Phys. Rev. C*, **106** (2022) 024902.
- [36] WOLTER H. *et al.*, *Prog. Part. Nucl. Phys.*, **125** (2022) 103962.
- [37] SORENSEN A. *et al.*, *Prog. Part. Nucl. Phys.*, **134** (2024) 104080.
- [38] DRISCHLER C. *et al.*, *Phys. Rev. Lett.*, **125** (2020) 202702.
- [39] TEWS I. *et al.*, *Neutron matter from local chiral EFT interactions at large cutoffs*, arXiv:2407.08979 [nucl-th] (2024).
- [40] JIANG W. G. *et al.*, *Phys. Rev. C*, **109** (2024) L061302.
- [41] PETSCHAUER S. *et al.*, *Front. Phys.*, **8** (2020) 12.
- [42] EVANS M. *et al.*, *A Horizon Study for Cosmic Explorer: Science, Observatories, and Community*, arXiv:2109.09882 [astro-ph.IM] (2021).